Catalysis Today 245 (2015) 155–162

Contents lists available at ScienceDirect

Catalysis Today

journal homepage: www.elsevier.com/locate/cattod

# Mesoporous silico-aluminophosphates derived from microporous precursors as promising catalyst for hydroisomerization

Rekha Yadav, Arvind Kumar Singh, Ayyamperumal Sakthivel*

*Inorganic Materials and Catalysis Laboratory, Department of Chemistry, University of Delhi, Delhi 110 007, India*

## ARTICLE INFO

*Article history:*
Received 30 November 2013
Received in revised form 14 August 2014
Accepted 16 September 2014
Available online 25 October 2014

*Keywords:*
Hydroisomerization
1-Octene
SAPO-37
SAPO-34
SAPO-5
Mesoporous silicoaluminophosphates
Faujasite
Secondary building units

## ABSTRACT

A series of mesoporous silicoaluminophosphates (MESO-SAPOs) with different silica contents were synthesized using the microporous precursors of SAPO-37 (MESO-SAPO-37). Various analytical and spectroscopic techniques revealed the presence of mesoporous and microporous properties of the materials. The resulting materials were applied to vapor-phase hydroisomerization of 1-octene to afford the corresponding branched alkenes in good yields under ambient conditions. The catalytic activity of MESO-SAPO-37 was compared to those of other mesoporous analogs obtained from SAPO-34 and SAPO-5 precursors. Among all the synthesized materials, MESO-SAPO-37 showed the best catalytic activity owing to the presence of faujasite units.

## 1. Introduction

Isomerization of linear alkanes/alkenes to the corresponding *iso*-alkanes/alkenes is an important transformation in terms of increasing the octane count of fuel. The process was developed during World War II to increase the octane number of gasoline [1] and is important in the petrochemical industry and fine chemical synthesis [2]. Earlier, isomerization reactions were carried out using homogeneous Friedel–Crafts-type acid catalysts [3]; however, these catalysts suffer from drawbacks such as handling difficulty, generation of a large amount of waste and its disposal, and regenerability of catalysts. These limitations can be overcome by replacing homogeneous catalysts with heterogeneous solid-acid catalysts, including zeolite, microporous aluminophosphate (AlPO), and other solid-acid catalysts [4–6]. Besides a heterogeneous phase, microporous solid-acid catalysts have several advantages such as ion exchange and high sorption properties; they also possess enhanced structural diversity in which Al can be substituted with different metal species to fine-tune interfacial acidity and catalytic properties [7–9]. The silica-substituted AlPOs, namely, SAPO-*n* (where "*n*" represents a distinct structure type), are relatively less acidic than zeolites [10] and provide mainly moderately acidic sites appropriate for isomerization reactions. The introduction of diverse metals to different SAPO-*n* systems afforded good isomeric yields [11–15]. However, these catalysts suffer from pore blockage and pore-size limitation for bulkier reactant molecules. The discovery of mesoporous materials containing pores with diameters between 2 and 50 nm [16–21] provided a new array of materials with large pore-size distribution. These materials showed good results in the fields of separation, adsorption, support, and heterogeneous catalysis [22–26].

In 1998, Montoya-Urbina et al. synthesized SAPO-5 system in presence of a surfactant, cetyltrimethylammonium bromide (CTAB), and reported better conversion for the isomerization of *m*-xylene compared to the systems synthesized without surfactant [27]. In continuation to the study, many researchers have tried to fine-tune the intrinsic properties of SAPO-*n* system by introducing surfactants during the synthesis and achieved good isomeric yields [28–31]. The surfactant-directed resulting materials are microporous with interparticle mesopores. In this regard, we recently synthesized a series of mesoporous SAPOs from microporous precursors to enhance the access to active sites [32–34]. Notably, faujasite-type aluminosilicates and SAPOs have great potential for use as fluid catalytic cracking (FCC) catalysts in gasoline upgrading and other isomerization reactions [13,35].

This study focuses on the faujasite-type SAPO-37 precursors assembled over surfactant assemblies for the synthesis of

---

* Corresponding author. Tel.: +91 8527103259.
*E-mail addresses:* sakthiveldu@gmail.com, asakthivel@chemistry.du.ac.in (A. Sakthivel).

http://dx.doi.org/10.1016/j.cattod.2014.09.026
0920-5861/© 2014 Elsevier B.V. All rights reserved.

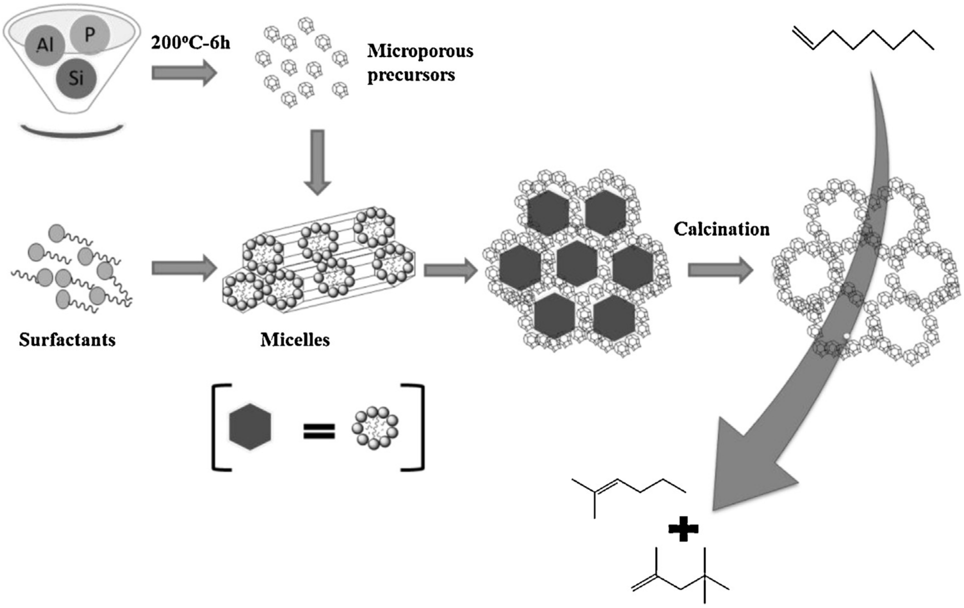

**Scheme 1.** Schematic representation for formation of MESO-SAPO-*n* from corresponding microporous precursors and its application on hydroisomerization of 1-octene.

mesoporous SAPOs (MESO-SAPO-37) as shown in Scheme 1. The detailed catalytic activity of these materials was compared for the vapor-phase hydroisomerization of 1-octene.

## 2. Experimental

### 2.1. Synthesis of materials

Pseudoboehmite (76% $Al_2O_3$; ACE, India), fumed silica (Aerosil-200; Sigma–Aldrich), orthophosphoric acid (85%, Merck), cetyltrimethylammonium bromide (99%; Spectrochem), 25 wt.% tetramethylammonium hydroxide in water (25 wt.%; Tritech chemical) and 40 wt.% tetrapropylammonium hydroxide in water (40 wt.%; Tritech chemical) were used in the synthesis.

A series of MESO-SAPO-37 with different silica contents was prepared as per the procedure described elsewhere [32]. The molar composition used for MESO-SAPO-37 synthesis was: 1.0$(TPA)_2O$; 2.1–2.8$(TMA)_2O$; 1.0 $Al_2O_3$; 1.0 $P_2O_5$; $x$$SiO_2$; 0.40–0.60 CTAB; and 226.94 $H_2O$, where $x = 0.43$, 0.50, 0.60 and 0.80. The synthesis of mesoporous silicoaluminophosphate involved two steps, where first step comprises the synthesis of microporous precursors and the second step involves assembly of the preformed microporous precursors into mesoporous silicoaluminophosphate in presence of a surfactant solution.

#### 2.1.1. Synthesis of microporous SAPO-37 precursor

The first step involved the formation of microporous SAPO-37 precursor as per the following procedure, with the molar gel composition 1.0 $Al_2O_3$:1.0 $P_2O_5$:0.43 $SiO_2$:1.0 $(TPA)_2O$:0.025 $(TMA)_2O$:50.0 $H_2O$. Solution A was prepared by slowly adding 5.25 g Pseudoboehmite alumina to a solution of 9.223 g of 85 wt.% phosphoric acid and 10 g of $H_2O$. The resultant solution was stirred for 8 h. Solution B was prepared by adding a calculated amount of fumed silica into the mixture containing an appropriate amount of tetramethylammonium hydroxide (TMAOH; 25 wt.%) and tetrapropylammonium hydroxide (TPAOH; 40 wt.%). Solution B was added drop-wise to solution A, and the final mixture was stirred for 24 h. The resultant homogeneous mixture was allowed to crystallize at 200 °C for 6 h to get SAPO-37 precursor containing microporous secondary building units. For comparison, completely crystallized microporous SAPO-37 was obtained by 22 h crystallization.

#### 2.1.2. Conversion of SAPO-37 precursor into MESO-SAPO-37

To assemble MESO-SAPO-37 from microporous SAPO-37 precursors, the latter was introduced into the surfactant solution at an appropriate concentration. An additional quantity of tetramethylammonium hydroxide (25 wt.%) was added to the above mixture and the resultant solution was allowed to age at 90 °C for 36 h to obtain MESO-SAPO-37. Mesoporous silicoaluminophosphate prepared with different amounts of silica (0.43, 0.50, 0.60 and 0.80 M) are represented as MESO-SAPO-37-0.43S, MESO-SAPO-37-0.50S, MESO-SAPO-37-0.60S and MESO-SAPO-37-0.80S, respectively. All the as-synthesized samples were calcined in air at 550 °C for 6 h to remove organic molecules. Similarly, MESO-SAPO-34 and MESO-SAPO-5, i.e. mesoporous silicoaluminophosphates assembled using corresponding microporous precursors of SAPO-*n*, were prepared as per the composition specified in Table 1.

### 2.2. Characterization

Powder X-Ray diffraction patterns of all the materials were collected on BrükerD8 diffractometer with Cu-K$\alpha$ radiation ($\lambda = 1.54184$ Å), between $2\theta$ range of 1.5° and 40°, with a scan speed and step size of 0.5°/min and 0.02° respectively. FTIR spectra were measured on PerkinElmer FTIR 2000 in 400–4000 $cm^{-1}$ range using KBr pellets. The textural properties of materials like surface area (BET, DFT), micropore area (*t*-plot method), pore volume (BJH) and pore size distribution (BJH, DFT and HK) were derived from $N_2$ adsorption–desorption measurements carried out at −196 °C using an automatic micropore physisorption analyzer (Micromeritics ASAP 2020, USA) after the samples were degassed at 300 °C for at least 10 h under $10^{-3}$ Torr pressure prior to each run. The morphology and size of the materials were further analyzed using a Phillips Technai $G^2$30 TEM operated at 300 kV.

The pyridine FT-IR spectra were collected with a Thermo Scientific Nicolet 6700 FTIR single beam spectrometer using a liquid nitrogen-cooled MCT detector. Pyridine vapor adsorption was carried out in a Harrick Scientific HVC-DR2 reaction chamber with a detachable ZnSe window dome mounted inside a Harrick DRA-2